Modeling of Photoinitiation of Thick Polymers Illuminated with Polychromatic Light

Alec Scranton, Nicole Stephenson, and Dane Kriks
University of Iowa
Department of Chemical and Biochemical Engineering
Iowa City, Iowa, 52242

INTRODUCTION

A number of investigators have recently reported theoretical descriptions of photoinitiation of thick systems illuminated with monochromatic light[1-4], and have found that the rate of photobleaching is non-uniform and resembles a wave front. For example, Terrones and Pearlstein[2] presented a complete and accurate unsteady state model describing the initiator consumption and optical attenuation for free radical photopolymerizations in perfectly photobleaching systems illuminated with monochromatic light (the absorption of light is described using a single absorption coefficient). These authors demonstrated that for the case in which only the photoinitiator absorbs at the initiating wavelength, and becomes completely non-absorbing upon photolysis (perfectly photobleaching) the resulting integro-differential equation could be solved analytically. Interestingly, Terrones and Pearlstein[3] found that with increasing initial absorbance, the local initiation rate becomes increasingly nonuniform, and, for high initial absorbance, assumes the form of a localized wave that propagates through the sample. In further contributions, Terrones and Pearlstein investigated the effect of the photoinitiation rate profiles on the subsequent polymerization.

In another study, Ivanov and Decker[4] solved the coupled differential equations that describe the spatial and temporal evolution of both the light intensity gradient and the initiator concentration gradient. Once again, only the initiator was assumed to absorbing, and the equations were solved analytically. These authors also assumed that initiation was by monochromatic light, and diffusion was neglected. The initiation kinetics were coupled to the polymerization kinetics using a quasi-steady-state approximation for bimolecular radical termination. The influence of sample thickness on the kinetics of the photoinitiator and monomer consumption was investigated for systems varying from transparent films to optically thick samples.

Recently Miller, *et al.*[1] generalized the governing differential equations to include the effects of absorption by the initiator fragments, absorption by the monomer, and diffusion of the initiator to further characterize the photoinitiation wave front as it traveled through the depth of the sample. In this case, the coupled differential equations could not be solved analytically, but rather were solved numerically using the method of finite differences. As expected, the photoinitiation rate resembled a wave with a local max at any given time throughout the depth of

the sample. It was also shown that initiator concentration and initiator absorbance must be measured separately due to the continuous change of optical density in the sample. All of the conclusions made by Miller, *et al.*[1] were done using monochromatic light.

In this contribution, we build upon the model reported by Miller, *et al.*[1] by generalizing the governing differential equations further to include the effects of polychromatic illumination. We present a model with encompasses the spectrum of wavelengths from 300 to 405 nm over which the initiator absorbs and include the effects of absorption by the initiator fragments, absorption of the products, and absorption of the monomer. The various simulations presented in this paper illustrate the different effects each variable has in the overall photoinitiation process.

GENERALIZED GOVERNING DIFFERENTIAL EQUATIONS

For an initially homogeneous sample subject to uniform illumination normal to the surface, the evolution of the light intensity gradient through the depth of the sample is dependent on the concentration of initiator, which also varies with sample depth and time. For the generalized case that includes the effects of absorption by the initiator fragments, absorption by the monomer, and initiator diffusion, the following set of coupled partial differential equations describes the light intensity and initiator concentration profiles for a polychromatic light source.

$$\frac{\partial C_i(z,t)}{\partial t} = -\frac{C_i(z,t)}{N_A h}\sum_j \frac{\varepsilon_{i,j}\phi_j I_j(z,t)}{\nu_j} + D_i\frac{\partial^2 C_i(z,t)}{\partial z^2} \quad (1)$$

$$\frac{\partial C_p(z,t)}{\partial t} = \frac{C_i(z,t)}{N_A h}\sum_j \frac{\varepsilon_{i,j}\phi_j I_j(z,t)}{\nu_j} + D_p\frac{\partial^2 C_p(z,t)}{\partial z^2} \quad (2)$$

$$\frac{\partial I_j(z,t)}{\partial z} = -\left[\varepsilon_{i,j}C_i(z,t) + A_{m,j} + \varepsilon_{p,j}C_p(z,t)\right]I_j(z,t) \quad (3)$$

In these equations:

$C_i(z,t)$ represents the initiator molar concentration at depth z and time t;

$C_p(z,t)$ represents the photolysis product molar concentration at depth z and time t;

j is the index that identifies the wavelength of light under consideration (the wavelengths between 300 and 405 nm were considered at 1 nm increments, therefore j ranged from 1 to 106);

$I_j(z,t)$ represents the incident light intensity at depth z and time t for wavelength j, with dimensions of energy/(area·time);

$\varepsilon_{I,j}$ is the initiator molar absorptivity at wavelength "j" with dimensions of volume/(length·mole);

$\varepsilon_{p,j}$ is the photolysis product molar absorptivity, with dimensions of volume/(length·mole) and accounts for the photon absorption by all fragmentation species;

N_A is avogadro's number;

h is Planck's constant;

ν_j is the frequency of light at wavelength j, with dimensions of inverse time;
ϕ_j is the quantum yield of the initiator at wavelength j, defined as the fraction of absorbed photons that lead to fragmentation of the initiator;
D_i is the diffusion coefficient for the initiator with dimensions of length^2/time;
D_p is the diffusion coefficient for the photolysis products; and
$A_{m,j}$ is the absorption coefficient of the monomer and the polymer repeat unit (the product of the molar absorptivity and the molar concentration of the monomer units), with dimensions of inverse length.

In these governing equations, division of the incident light intensity I(z,t) by the product $N_A h\nu$ simply converts the intensity to the photon flux, with dimensions of moles of photons per unit area per unit time. Note that in equation 1, the change in initiator concentration with time includes one contribution from consumption of initiator in the photochemical reaction (the first term, which includes a sum over all incident wavelengths) and a second contribution from the diffusion of the initiator that arises from the resulting concentration gradient. Similarly, equation 2, which describes the initiator products (fragments), has one contribution accounting for the production of the fragments in the photochemical reaction (again a sum over all wavelengths), and a second for diffusion. Finally, the light intensity profile through the depth of the sample for each incident wavelength is represented in equation 3 (106 such equations were solved simultaneously), which includes terms arising from the absorbance by the initiator, monomer, and the photolysis products. Note that any change in the monomer absorption coefficient upon polymerization has been neglected in the development of the governing differential equations. The following boundary conditions and initial conditions apply to this system:

$$C_i(z,0) = C_o \quad (4)$$

$$C_p(z,0) = 0 \quad (5)$$

$$\frac{\partial C_{i,p}}{dz} = 0 \text{ at } z = 0 \text{ and } z = z_{max} \text{ (the thickness of the sample)} \quad (6)$$

$$I_j(0,t) = I_{oj} \quad (7)$$

Equation 4 accounts for the fact that the initiator concentration is initially uniform through the depth of the sample. Equation 5 indicates that photolysis product concentration is initially equal to zero throughout the sample, while equation 6 represents the no-flux boundary condition at the ends of the sample for both the initiator and the fragments (this boundary condition is necessary due to the diffusional terms in the governing equations). Finally, equation 7 indicates that the light intensity at the exposed surface is equal to the incident light intensity at all times.

RESULTS AND DISCUSSION

In the remainder of this paper, equations 1 through 7 are solved simultaneously to demonstrate the effect of polychromatic illumination. Several simulations are shown in which one variable is changed and all others are held constant. The simulation conditions were selected to illustrate the effects of the concentration gradient, light intensity gradient, molar absorptivity, and quantum yield of the initiator, and the absorptivity of the initiator fragments, with the goal of identifying selection criteria for effective photopolymerization of thick systems.

Representative Simulation Results

The governing differential equations (equations 1–7) were solved numerically using the method of finite differences to obtain profiles of the light intensity, initiator concentration, and initiation rates as function of time, depth, and wavelength. For accurate results, a finite difference mesh size of 0.5 seconds in the time domain and 0.020 cm in the depth domain was chosen. The summation of wavelengths is calculated in 1 nm increments. Experimental data were drawn from a 200 W mercury-xenon lamp. Intensity and absorbance profiles were taken in 1 nm increments as shown in Figure 1 and all of the simulations were computed from the 300 nm to the 405 nm wavelength region. To verify the accuracy of the numerical method, the numerical solution was compared to the results provided by the monochromatic light simulation as computed by Miller et al.[1] for the case of no diffusion and no absorption by the initiator fragments and monomer. The individual wavelength results matched exactly to those of the monochromatic simulation done by Miller and the monochromatic data profile had a correlation of fit (R^2) for a comparison of the initiator concentration profiles that was greater than 0.994 as indicated by the analytical solution of Terrones and Pearlstein[2].

Figure 1 identifies the absorbance and intensity for BAPO with a molar concentration of 2.65×10^{-4} M. From this data set initiator extinction coefficients and an initial surface intensity for each individual wavelength can be calculated.

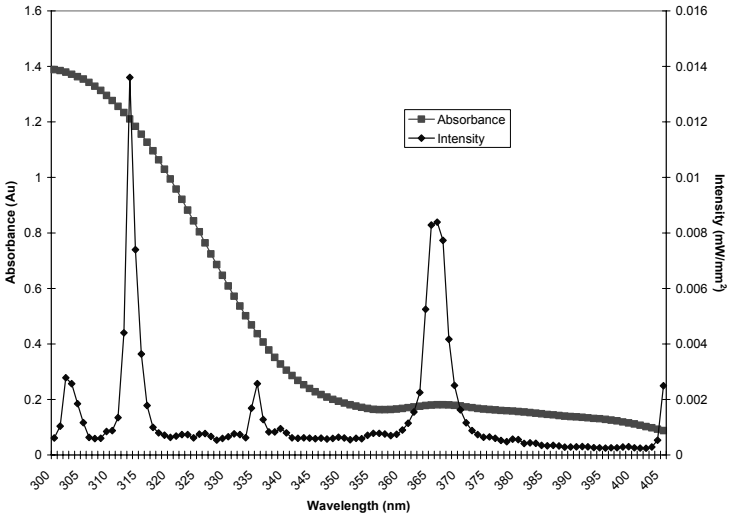

Figure 1. The absorption of 2.65×10^{-4} M BAPO compared to the normalized intensity of a 200 W Mercury lamp.

Figure 2a shows the local total intensity from waves 300 nm to 405 nm as a function of sample depth. For this set of simulation conditions, the transmittance of the sample reaches a normalized value of 0.9 in 105 seconds, and a normalized value of 0.99 in 119 seconds.

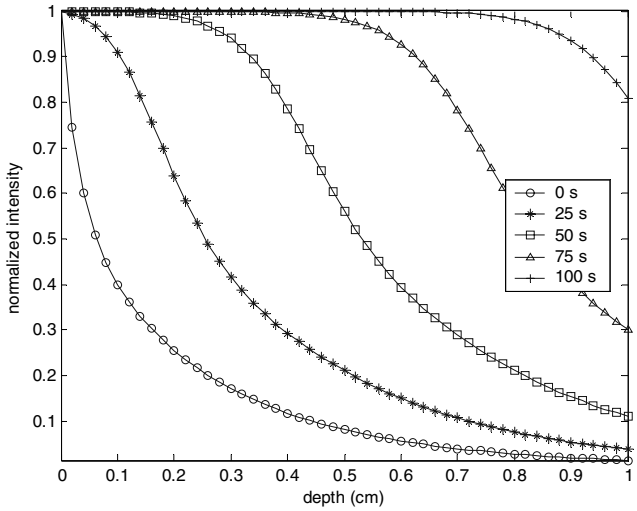

Figure 2. Time and depth dependence of the normalized light intensity in a 1.0 cm sample. The total light intensity is 1.3971 mW/mm^2, C_0 is 2.38 g/L (0.2 wt %), Φ is 0.2, and ε_p is 0 L (mol cm)$^{-1}$. Mesh sizes are 0.5 s and 0.020 cm.

As the light penetrates deeper into the sample with time the initiator concentration decreases as seen in Figure 3. These families of curves demonstrate a sigmoidal shape of the total intensity plot, which is in general agreement to the trend observed for monochromatic light.

Effect of Initiator Concentration

Figure 4a-d illustrates the effect of the initial initiator concentration on the evolution of the light intensity gradient in a photobleaching sample. This figure includes light intensity profiles for four different initial initiator concentrations at four different times, with all other simulation parameters being equal. As with monochromatic light, the multi-wavelength illumination exhibits a more rapid photobleaching at the lowest initiator concentration. For example, after 50 seconds of polychromatic illumination, the systems with initial initiator concentrations of 0.1 wt%, 0.2 wt%, 0.3 wt%, and 0.4 wt% exhibit a normalized intensity of 80% at depths of 0.880 cm, 0.420 cm, 0.260 cm, and 0.140 cm, respectively.

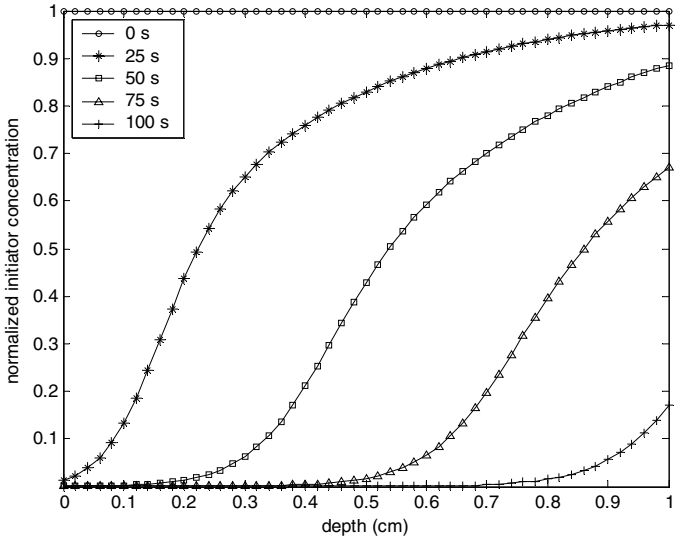

Figure 3. Time and depth dependence of the normalized initiator concentration in a 1.0 cm sample. The total light intensity is 1.3971 mW/mm^2, C_0 is 2.38 g/L (0.2 wt %), Φ is 0.2, and ε_p is 0 L (mol cm)$^{-1}$. Mesh sizes are 0.5 s and 0.020 cm.

Figure 5a-d illustrates the effect of the initiator concentration on the profiles of the initiation rate as a function of depth. Assuming that two active centers are produced upon fragmentation of the initiator, the instantaneous local rate of production of free radicals, $R_i(z,t)$, is represented by the following equation.

$$R_i(z,t) = 2\phi\varepsilon_i C_i(z,t) I(z,t) \qquad (8)$$

Using this equation, the photoinitiation rate, $R_i(z,t)$, may be calculated directly from $C_i(z,t)$ and $I(z,t)$ profiles obtained by the numerical solution of equations 1 through 7. $I(z,t)$ is the total sum of the intensity from each wavelength at a specific depth and time. Figure 5a-d contains profiles of the photoinitiation rate as a function of depth for the same conditions shown previously in Figure 4. The trends, in general, are similar to that of monochromatic light. At a given time the initiation rate increases to a maximum and then decreases due to lack of intensity. This polychromatic incident light contains both high and low initiator absorptivities, and thus has a wider breadth wave front as compared with that of monochromatic light. Wavelengths with higher absorptivities do not penetrate into the sample, but instead absorb more photons at the surface while wavelengths with lower absorptivities penetrate deeper into the sample but do not absorb as many photons.

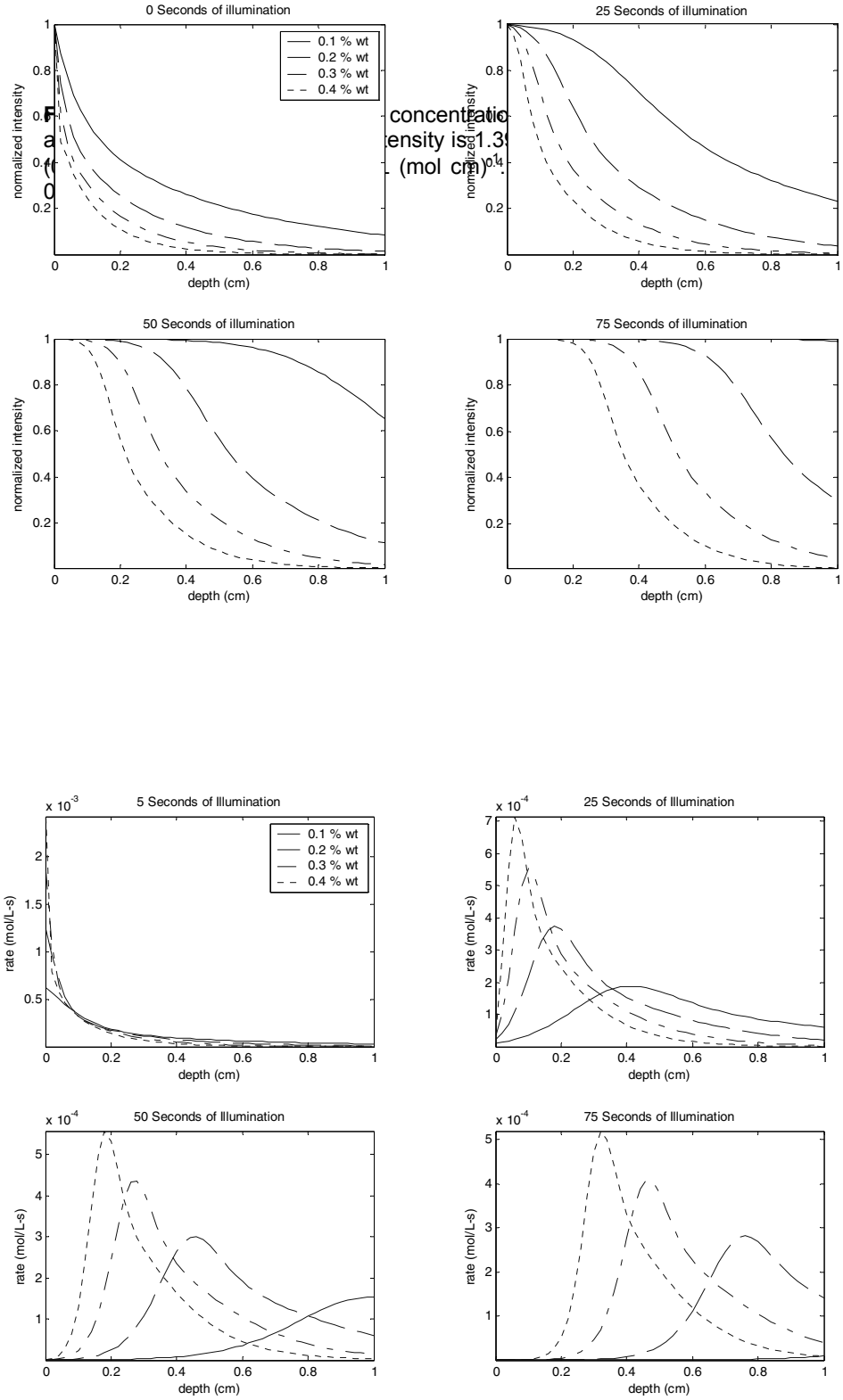

Figure 5. Effect of various initiator concentrations on the photoinitiation rate in a 1.0 cm sample. The total light intensity is 1.3971 mW/mm^2, C_0 is 2.38 g/L (0.2 wt %), Φ is 0.2, and ε_p is 0 L (mol cm)$^{-1}$. Mesh sizes are 0.5 s and 0.020 cm.

Effect of the Molar Absorptivity of the Initiator

The molar absorptivity is dependent on wavelength as shown in Figure 1. For these simulations, the molar absorptivity of each wavelength was changed by a common factor of ½ for one simulation and a factor of 2 for another. Figure 6a-d shows that as the initiator molar absorptivity increases, the maximum initiation rate increases, the breadth of the propagating front decreases, and the rate of spatial propagation through the sample increases. A low molar absorptivity allows more efficient penetration of light into the sample; however, a higher molar absorptivity leads to higher rates of photon absorption, higher rates of spatial propagation, and higher rates of initiation. Figure 6 illustrates more clearly that it is advantageous to have a system with relatively high initiator absorptivity, as this leads to a locally high rate of initiation that will lead to a higher local rate of polymerization, beginning on the surface. While single wavelength illumination displayed a slower rate of spatial propagation when there is higher initiator absorption, multi-wavelength illumination displays a higher rate of spatial propagation through the thickness of the sample. These results clearly show an advantage for multi-wavelength illumination for initiators with high molar absorptivity.

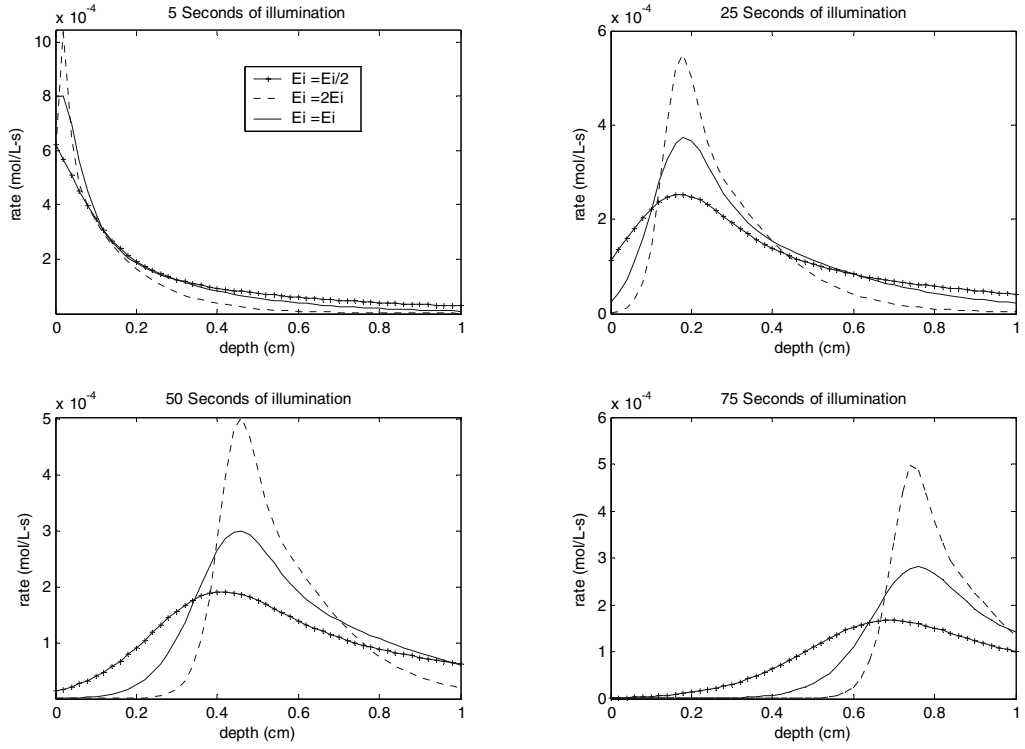

Figure 6. Effect of various initiator absorptivities on the photoinitiation rate in a 1.0 cm sample. The total light intensity is 1.3971 mW/mm^2, C_0 is 2.38 g/L (0.2 wt %), Φ is 0.2, and ε_p is 0 L (mol cm)$^{-1}$. Mesh sizes are 0.5 s and 0.020 cm.

Effect of the Photolysis Product Absorptivity

To analyze the product absorpitivity, a data set was constructed in relation to the initiator absorptivity for each wavelength. The values were chosen as follows: ε_p = 0 (L/mol·cm), which corresponds to perfect bleaching, $\varepsilon_p = \varepsilon_i/5$, which corresponds to intermediate bleaching and $\varepsilon_p = \varepsilon_i$, which corresponds to a minimal or non-bleaching system. At time zero (Figure 7a) all the intensity gradients are initially equal because there are no photolysis products. As time progresses, the system with perfect bleaching experiences a higher intensity gradient as a function of depth as compared to that of intermediate and non-bleaching systems. The non-bleaching system stays stagnant as time progresses. In the intermediate and non-bleaching cases, an assumption was made that the photolysis products absorb in proportion to the initiator absorptivity at all wavelengths in the 300 nm to 405 nm region. However, the actual photolysis product will have its own absorbance spectrum, so initiators should be chosen such that the products of photolysis are non-absorbing in the region of the spectrum where the initiator absorbs.

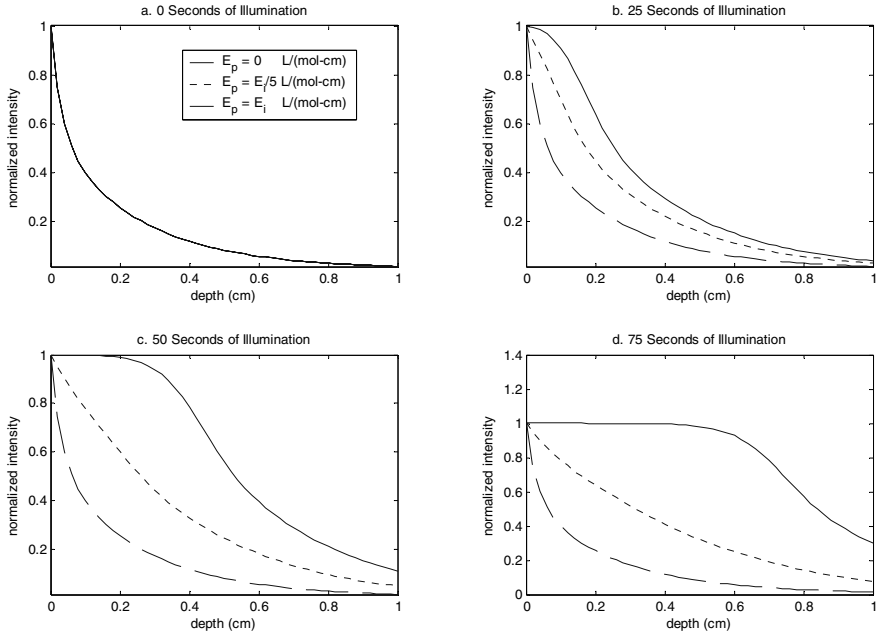

Figure 7. Effect of photolysis product absorptivity on the intensity profile in a 1.0-cm sample. The total light intensity is 1.3971 mW/mm^2, C_0 is 2.38 g/L (0.2 wt %), Φ is 0.2, and ε_p is 0 L (mol cm)$^{-1}$. Mesh sizes are 0.5 s and 0.020 cm.

CONCLUSIONS

Simulation results have shown that the initiator concentration has an optimum value, corroborating an experimentally observed trend.[1-2] The ability to have both high and low initiator absorptivities has proven to be a key advantage when using a polychromatic light source. High initiator absorptivity at one or more wavelengths allows for a higher maximum rate of initiation near the surface, while a lower absorptivity at a different wavelength allows initiation to occur deeper in the sample. The combined effects of all the incident wavelengths in the polychromatic light leads to the more rapid and efficient photoinitiation wave front propagation through the depth of the sample than that observed using monochromatic light. Also demonstrated was that in any system where an element is absorbing over the same wavelengths as the initiator, initiation will be hindered. The wave front of the perfectly non-bleaching system did not propagate through the depth of the sample and remained stagnant, while the other two systems under consideration eventually reached the bottom of the sample.

This modeling approach for obtaining the photoinitiation rate profiles is very versatile and can be used to obtain a detailed picture of how a variety of variables affect the spatial variations in the initiation rate. For example, in addition to the variables that have been illustrated here, the model can be adapted for any photoinitiator/monomer/additive system of interest.

REFERENCES

1. G. A. Miller, L. Gou, V. Narayanan, and A. B. Scranton, *J. Polym. Chem.* 40,793 (2002)
2. Terrones, G.; Pearlstein, A.J. *Macromolecules*; 2001; 34, 3195-3204
3. Terrones, G.; Pearlstein, A.J. *Macromolecules*; 2001; 34, 8894-8906
4. Ivanov, V.V.; Decker. C. *Polymer Int*. 2001, 50, 113-118